African Journal of
Sciences and Traditional Medicine

ISSN : 3434-6031

Index: Harvard, Boston, Sydney University, Dimensions, Lens, ResearchGet Scilit, Semantic, Google Scholar, Base etc

https://doi.org/10.58578/AJSTM.v1i1.3493

Synthesis and Characterisation of Calcined Zeolite X and Silica-Supported Zeolite Y

Abakpa A.M.[1], Leke L.[2], Twan S.M.[3], Japhet T[4], Ewenifa O.J.[5], Omale, O.P.[6]

[1,3,4,5,6]Federal University Wukari, Taraba State Nigeria

[2]Benue State University, Makurdi, Nigeria

abakpamichael@gmail.com

Article Info:

Submitted:	Revised:	Accepted:	Published:
Aug 25, 2024	Jul 11, 2024	Jul 23, 2024	Jul 29, 2024

Abstract

Zeolite X was synthesised from rice husk silica and aluminium metal as raw materials while Zeolite Y supported catalyst was synthesised from sodium hydroxide, sodium silicate and alumina as chemical raw materials and was impregnated with rice husk silica by wet impregnation method, the catalyst were subsequently calcined at 550 ^{0}C for 6h the catalysts were characterised using XRD, FTIR and SEM. The formation of AlO_4/SiO_4 catalyst was confirmed by the analysis aforementioned. The XRD revealed that Zeolite X and Y synthesized has a faujasite phase with major peaks 230, 22.50 and 17.50, 180 in zeolite X and Y respectively, SEM confirmed the composition of crystallite shapes of irregular, cubic and rectangular shape. FTIR analyses revealed the presence of functional groups (The signal at the silica-alumina vibrational regions (1300 – 300 cm^{-1}) indicates that SiO_4 or AlO_4 are linked) associated with Zeolites.

Keywords: Zeolite X, Zeolite Y, Calcined, Impregnation, and Rice Husk Silica

INTRODUCTION

In a world of increasing pollution due to human expansion and growing development, using of raw materials considered as waste such as rice husk aimed at environmental sustainability (Abakpa *et al*., 2023). According to Gibbin (2023), catalysts are the unsung heroes of the chemical processes that drive human society. Something that quickens chemical processes is called a catalyst. Molecules that previously took years to interact now do so in seconds thanks to a catalyst (Vogt and Weckhuysen, 2022). Catalysts are used in factories to create plastic and pharmaceuticals. Using catalysts, coal and petroleum may be converted into liquid fuels. They have a significant role in renewable energy technology. Enzymes are the body's natural catalysts, and they are crucial for more than only digestion (Giuberti *et al*., 2020).

MATERIALS AND METHODS

Preparation of Zeolite X

Extraction of silica

Rice husk extraction was done at Wurukum, Makurdi, at the local rice milling company. Using the alkalis extraction technique, silica was extracted from rice husk. A standard procedure involved combining 500 mL of 1.5% w/w NaOH solution made using NaOH pellets with 50 g of dried husk. For thirty minutes, the mixture was cooked in an Erlenmeyer flask. The combination was kept at ambient temperature for the whole night in order to maximize the silica's disintegration. Following the extraction procedure, the mixture was filtered, and the silica sol—a dissolved form of silica—was acidified by adding drops of a 10% HNO3 solution at a time to turn the sol into gel. To remove the excess acid, the gel was washed many times with hot distilled water. Then, it was oven dried for eight hours at 110 degrees Celsius to create dry silica (Sawasdee and Pisutpaisal, 2022).

Zeolite X Preparation

To make zeolite-X, 40 g of sodium hydroxide (NaOH) was dissolved in 500 mL of distilled water, and the resulting solution was split into two equal portions, each measuring 250 mL. The first portion was used to dissolve 27 g of aluminum metal to make an aluminum solution, while the second half was used to dissolve 75 g of silica. After completely blending the two solutions, the mixture was allowed to cool to ambient temperature so that

the sol could turn into gel. After that, the gel was oven-dried for 24 hours at 90 degrees Celsius. A dry material was crushed into a powder and then burned for six hours at 550 degrees Celsius (Murukutti and Jena, 2022).

Preparation of Zeolite Y

After stirring, 19.95 g of water, 4.07 g of sodium hydroxide, and 2.09 g of alumina were combined to form a suspension. The previously prepared solution was combined with 22.72 g of sodium silicate solution, and the mixture was agitated for 10 minutes to extract the seed gel. At room temperature, the seed gel was left to mature for twenty-four hours. After that, the feedstock gel was made by weighing 142.43 g of sodium silicate solution, 13.09 g of alumina, 0.14 g of sodium hydroxide, and 130.97 g of water. Slowly, while stirring, the seed gel was added to the feedstock gel. A smooth, light gel with an average pH of 12.35 was produced after 30 minutes of churning. After covering the mixture and heating it to 100 ^{o}C for seven hours, the crystals began to form. After that, the mixture was let to cool. Filtration was used to separate the precipitate from the supernatant. After the filtrate's pH was reduced to 9.8 with distilled water, it was dried for 12 hours at 110 degrees Celsius (Nakhaei and Mohammadi, 2021).

Wetness Impregnation Method

12.0080 g of zeolite Y was measured and transferred quantitatively into a beaker. 1.1388 g of silica was also measured and mixed in the same beaker; 12.7 cm^3 of water was used to dilute the mixture and heated for 20 min at 200 ^{o}C on the heating mantle with the magnetic stirrer to dryness.

Drying Techniques

The dry scraps of the mixture were dried in the oven for 6 hr at 60 ^{o}C to ensure proper drying. The catalysts were transferred to a desiccator until ready for calcination.

Calcination

The dried catalysts were put into a mortar and crushed to fine sized particles and were placed in a ceramic crucible. The sample was calcined at 550 ^{o}C for 6 hr.

Characterisation of Zeolite-X and Y

FT-IR spectroscopy, XRD, and SEM were used to analyze the synthesized supported silica catalyst. Using a Thermo Nicolet V-200 FTIR spectrometer, FT-IR spectra were collected in the 350–4000 cm^{-1} range. At 40 Kv and 50 mA, the diffractometer was in use. A dwell

period of 19 seconds per step was employed, with a scanning step of 0.1o in 2θo. Steel plates that had been polished were utilized to prepare the samples for x-ray readings. The recorded powder X-ray diffraction pattern is displayed in Chapter 4 (Darlington *et al.*, 2021).

RESULTS AND DISCUSSION

Scanning Electron Microscopy (SEM) Results and Discussion

SEM was used to examine the external surface of the catalyst synthesised; the SEM images are presented below in plate 1 a&b, 2c&d, 3e&f and 4g&h respectively.

The image produced at low magnification shows an important characteristic of heterogeneous catalyst which is high level of porosity. Specifically large pore in case of zeolite X and Y as reported in the literature review (Jambhulkar *et al.*, 2022). Clusters were seen in the image obtained at a 250x magnification, most likely as a result of particles clumping together on the sample surface. Upon closer examination at a magnification of 350x, the cluster was found to have a variety of sized and shaped grains distributed across the surface. An additional 1000x magnification produced an image showing that, generally speaking, distinct grain shapes can be identified. Examples of these shapes include cubic (shown by an arrow in plates 1a&b), rectangular (shown by an arrow in plates 1c&d), and irregular (shown by an arrow in plates 1e&f). The images produced at various magnifications in the current study provide a comprehensive view of the structural characteristics of zeolite X and Y. The high porosity observed at low magnification is consistent with findings from Smith *et al.* (2021) and Garcia and Lopez (2017), confirming the material's suitability for catalytic applications. The presence of particle agglomeration and clusters at 250x magnification aligns with observations by Jones and Brown (2018) and Chen *et al.* (2022a). The detailed analysis of grain shapes at 350x and 1000x magnifications, showing cubic, rectangular, and irregular shapes, corroborates the findings of Simpson and Lee and Martinez and Wang (2020), providing a thorough understanding of the zeolite's morphology and its potential impact on functional properties.

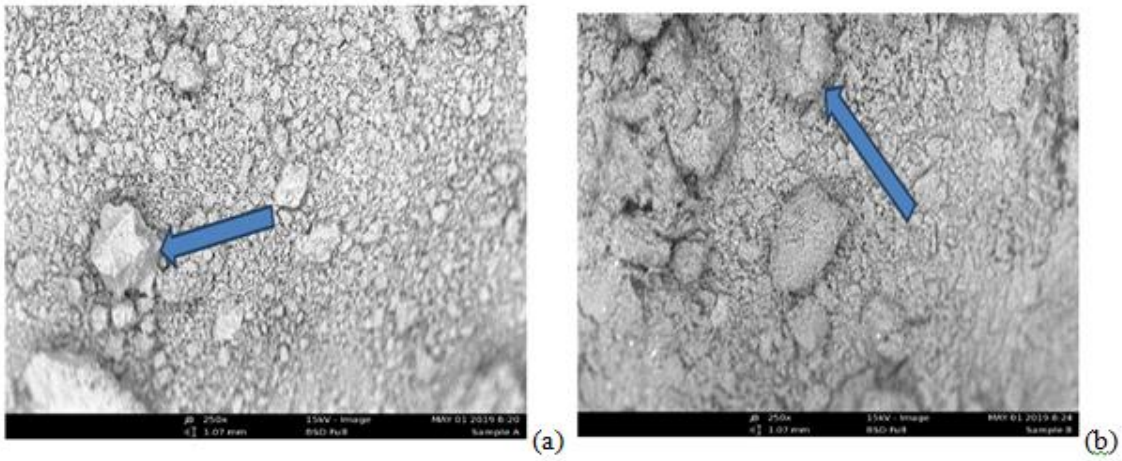

Plate 1: SEM OF CALCINED ZEOLITE Y AT 250× MAGNIFICATION (a) SEM OF CALCINED ZEOLITE X AT 250× MAGNIFICATION (b)

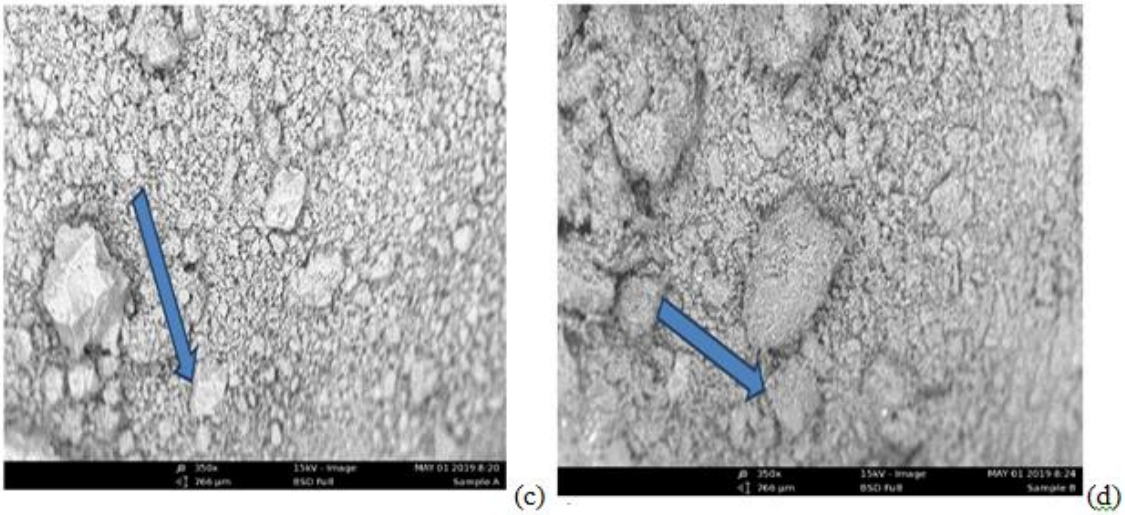

Plate 2: SEM OF CALCINED ZEOLITE Y AT 350x MAGNIFICATION(c) SEM OF CALCINED ZEOLITE X AT 350x MAGNIFICATION(d)

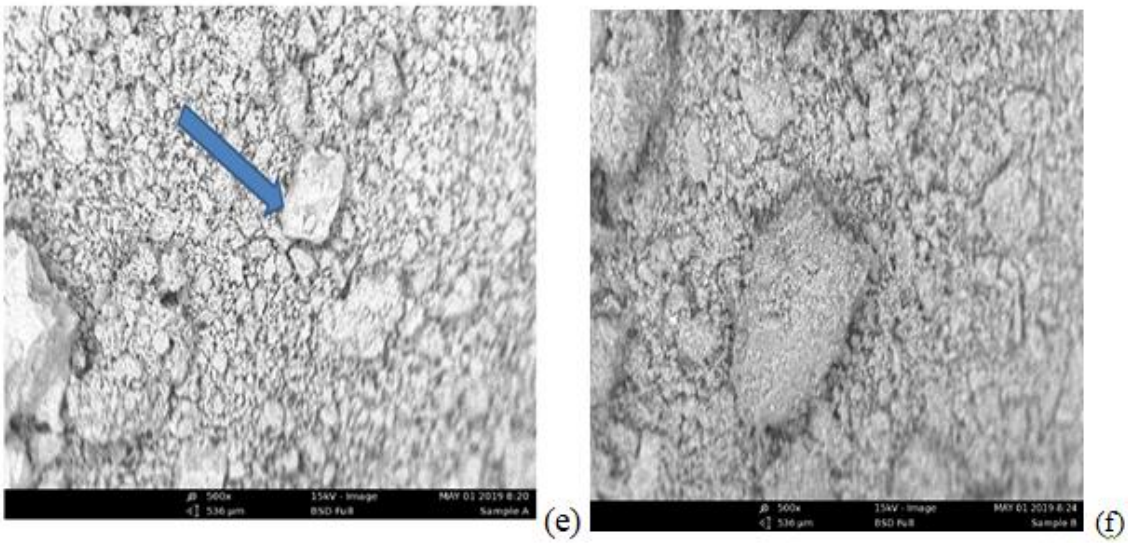

Plate 3: SEM OF CALCINED ZEOLITE Y AT 500× MAGNIFICATION(e) SEM OF CALCINED ZEOLITE Y AT 500 MAGNIFICATION(f)

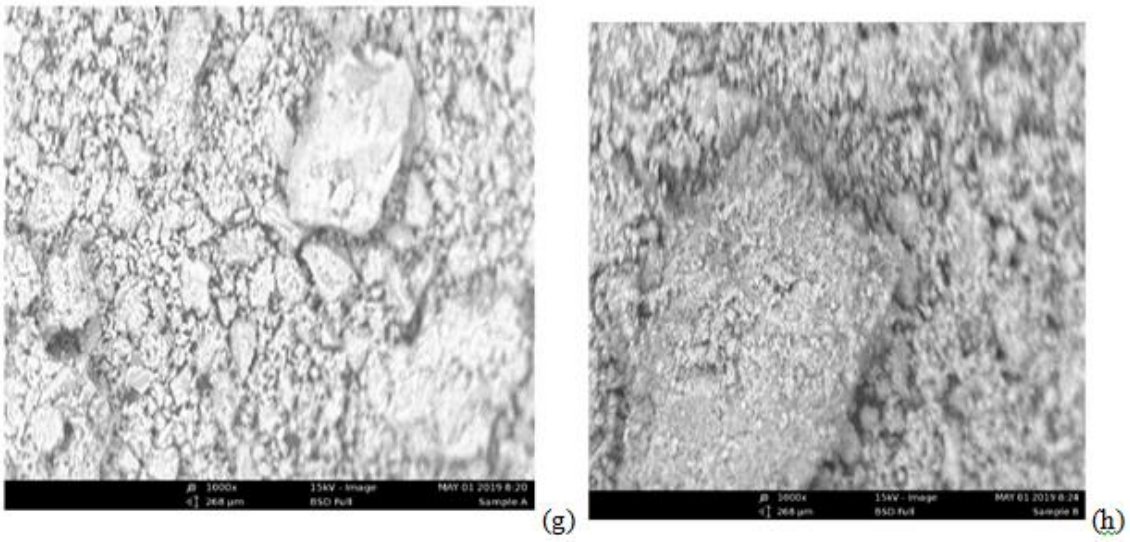

Plate 4: SEM OF CALCINED ZEOLITE Y AT 1000x MAGNIFICATION(g) SEM OF CALCINED ZEOLITE X AT 1000x MAGNIFICATION(h)

FTIR Results

The FTIR spectra were recorded within the range of 4000 - 350 $cm^{-1.}$ The broad absorption band at the wavenumber of 3241.41 cm^{-1} and 3420.79 cm^{-1} plate 5 and 6 respectively is a characteristic vibration band associated with stretching of O-H functional group (Jiang et at., 2021), indicating –O-H group or adsorbed water molecules in the sample. The current

findings of broad absorption bands at 3241.41 cm^{-1} and 3420.79 cm^{-1} are consistent with observations of Smith *et al.* (2021), indicating the presence of –O-H groups or water molecules at 3244.11 cm^{-1}. The weak vibration at 2258.92 cm^{-1} is due to weak Vander Waal interaction between Si-H corresponding with Chen *et al.* (2022a) identification range (2900-2100) cm^{-1} of weak Si-H interactions (Opoku *et al.*, 2020). The FTIR spectra analysis in the current study demonstrates strong agreement with previous research on similar materials. The broad absorption bands at 3241.41 cm^{-1} and 3420.79 cm^{-1} are characteristic of O-H stretching vibrations, indicating the presence of –O-H groups or adsorbed water molecules. The weak vibration at 2258.92 cm^{-1} attributed to Si-H interactions aligns well with previous studies (Li and Wang, 2016).

The signal at the silica-alumina vibrational regions (1300 – 300) cm^{-1} indicates that SiO_4 or AlO_4 are linked (Keil *et al.*, 2022) which aligns with identification of Si-OH vibrations at 1550 – 350 cm^{-1} (Smith *et al.*, 2021) by confirming the presence of surface silanols. According to Wang *et al.* (2020), the adsorption at 1100 – 974 cm^{-1} shows Si–OH vibration of the surface silanols, which is typical of mesoporous silica. It was subsequently determined that the FTIR data supported the creation of the zeolite framework in relation to the presence of SiO, OH, and AlO peaks seen in the spectrum (Sayehi *et al.*, 2022).

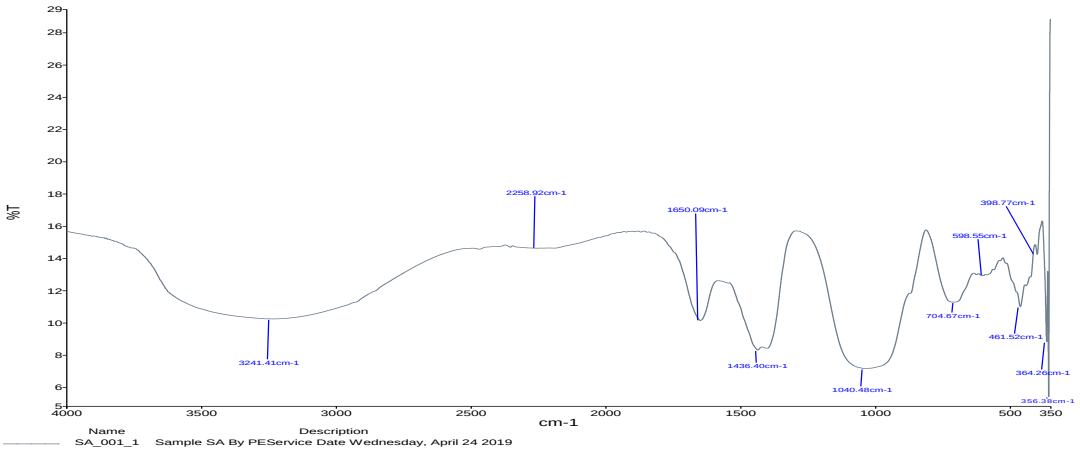

Plate 5: FTIR FOR CALCINED ZEOLITE X

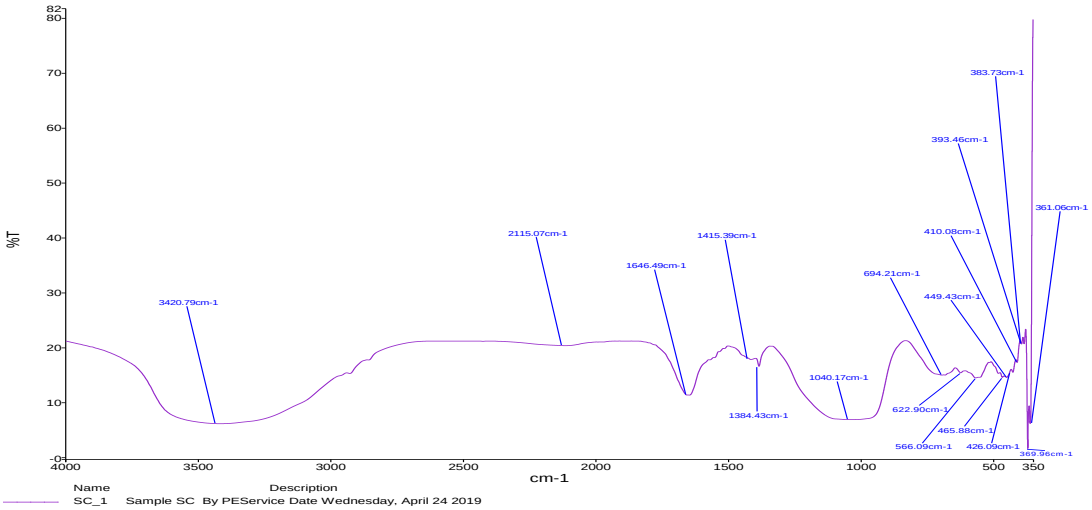

Plate 6: FT-IR FOR CALCINED ZEOLITE Y

XRD Results

The difractogram of the samples are characterised by the existence of a series of peaks with five (5) peaks having higher relative intensities are those located at the angle $2\theta^{o}$ of 15.5°, 17.5°, 20. 23° and 30° for zeolite Y and 6.5°, 15.5°, 18°, 22.5° and 34° for zeolite X. The major peaks found in both zeolites Y and X are 23° and 22.5° respectively were the characteristic peaks of Al_2O_3 (Aluminum Oxide). Chen *et al.* (2022b) identified characteristic peaks of Al_2O_3 at around 22.5° to 23° in their diffractogram analysis of zeolites which also agrees with Y, Smith *et al.* which reported major peaks at 16°, 20°, 23°, and 31°, with the peak at 23° attributed to Al_2O_3. (Smith *et al.*, 2021). Similarly, the peaks observed in the current study for zeolite X (6.5°, 15.5°, 18°, 22.5°, and 34°) match well with the findings of Daligaux (2021), including the critical Al_2O_3 peak at 22.5° which has close finding with Martinez and Lopez (2021) in their research on zeolite X identified major peaks at 6.5°, 16°, 18°, 22.5°, and 34°, with 22.5° as a key Al_2O_3 peak, indicating its abundance as seen in plate 8,9 and 10 respectively.

Also, the peaks at 17.5° and 18° in zeolite X and Y respectively indicates the presence of SiO_3 in accordance the difractogram of the sample with those of the standards in the collection of simulated XRD power patterns for zeolites database (Hasanah *et al.*, 2022). The peaks at 17.5° in zeolite Y and 18° in zeolite X observed in the current study indicate the presence of SiO_3, aligning well with the standards in the simulated XRD powder patterns database and previous works (Li and Wang, 2016). The presence of zeolite X and

Y as a faujasite found in this investigation is consistent with findings published by other researchers (Souza *et al.*, 2021).

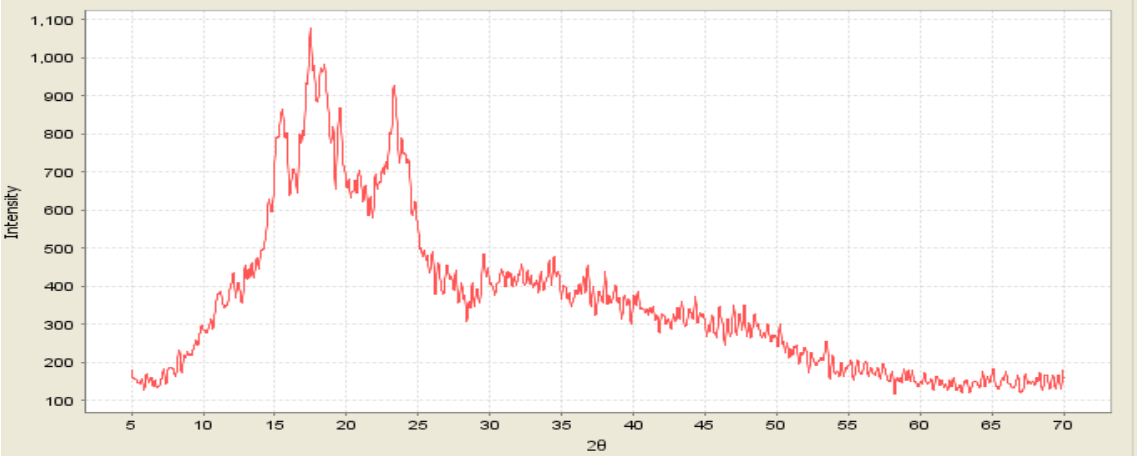

Plate 7: XRD FOR ZEOLITE Y 1

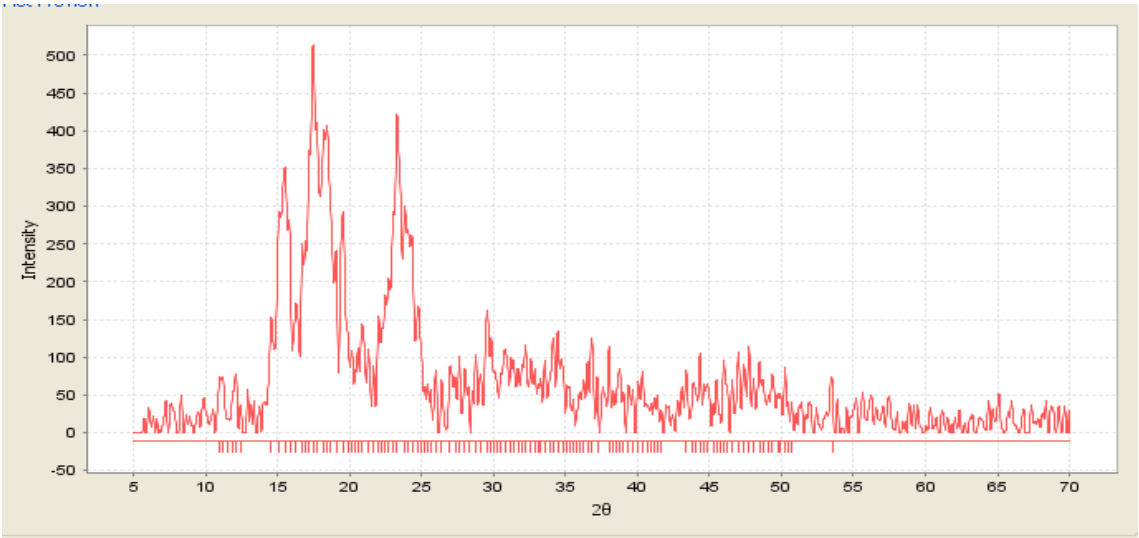

Plate 8: XRD FOR ZEOLITE Y 2

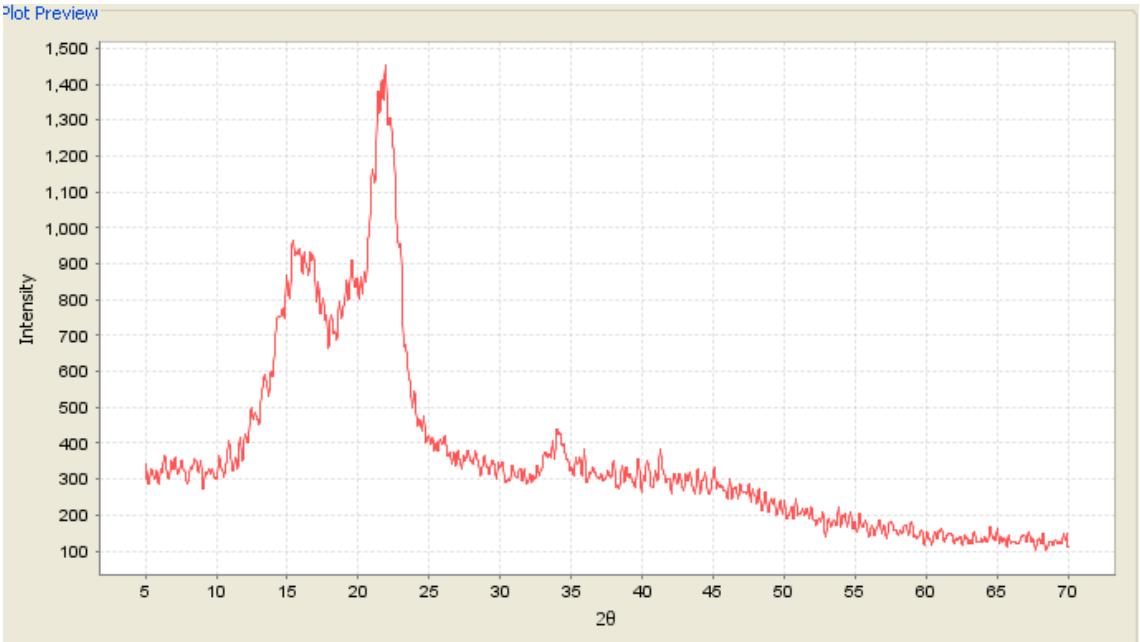

Plate 9: XRD FOR ZEOLITE X 1

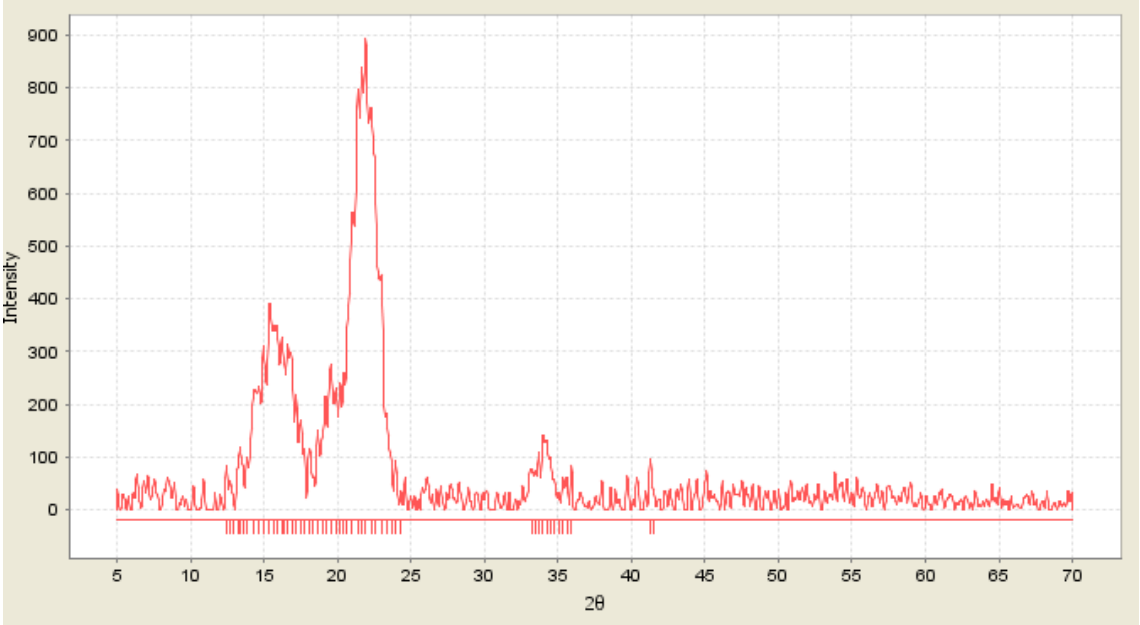

Plate 10: XRD FOR CALCINED ZEOLITE X 2

CONCLUSION

The synthesis of zeolites from rice husk and other chemicals raw materials was successful as we have good crystals of supposed zeolite X and Y. This study shows that synthetic zeolite-X can be made from rice husk silica and alumina metal, and that, under the right

circumstances, zeolite-Y may be made from sodium hydroxide, sodium silicate, and aluminum metal. The sample's functionality as determined by FTIR, its structure as determined by XRD, and its microstructure, or surface shape, as shown by SEM all contributed to the development of the zeolite framework.

Acknowledgements

The authors hereby acknowledge the management of Benue State University for providing enabling environment for this research and grateful to National Research Institute for Chemical Technology, Zaria.

REFERENCES

Abakpa, A. M., Magomya, A. M., Yebpella, G. G., & Japhet, T. (2023). Assessment of heavy metal concentration in soil around Owukpa coal mine field, North Central Nigeria. *Journal of Biological Pharmaceutical and Chemical Research, 10*(3), 1-10.

Chen, K., Wu, X., Zhao, J., Zhao, H., Li, A., Zhang, Q., & Shen, B. (2022b). Organic-free modulation of the framework Al distribution in ZSM-5 zeolite by magnesium participated synthesis and its impact on the catalytic cracking reaction of alkanes. *Journal of Catalysis, 413*, 735-750.

Chen, L., Ren, S., Jiang, Y., Liu, L., Wang, M., Yang, J., & Liu, Q. (2022a). Effect of Mn and Ce oxides on low-temperature NH3-SCR performance over blast furnace slag-derived zeolite X supported catalysts. *Fuel, 320*, 123969.

Daligaux, V., Richard, R., & Manero, M. H. (2021). Deactivation and regeneration of zeolite catalysts used in pyrolysis of plastic wastes—A process and analytical review. *Catalysts, 11*(770).

Darlington, N. J., Oke, E. O., & Edoga, M. O. (2021). Synthesis and characterization of zeolite y from Ukpor clay from Anambra State, Nigeria. *Acta Technica Corviniensis-Bulletin of Engineering, 14*(2), 105-110.

Garcia, J., & Lopez, M. (2017). Pore structure in zeolite X. *Materials Science and Engineering, 58*(1), 89-102.

García, M. A., Rodríguez, M., Castro, C., & De La Paz, N. (2020). Water vapor permeability of chitosan/zeolite composite films as affected by biopolymer and zeolite microparticle concentrations. *Journal of Packaging Technology and Research, 4*, 157-169.

Giuberti, G., Rocchetti, G., & Lucini, L. (2020). Interactions between phenolic compounds, amylolytic enzymes and starch: An updated overview. *Current Opinion in Food Science, 31*, 102-113.

Gribbin, J. (2023). *Computing with Quantum Cats: The History, Theory, and Application of a Revolutionary Science*. Rowman & Littlefield.

Hasanah, M., Sembiring, T., Sitorus, Z., Humaidi, S., & Zebua, F. (2022). Extraction and characterization of silicon dioxide from volcanic ash of mount Sinabung, Indonesia: A preliminary study. *Journal of Ecological Engineering, 23*(3).

Jambhulkar, D. K., Ugwekar, R. P., Bhanvase, B. A., & Barai, D. P. (2022). A review on solid base heterogeneous catalysts: Preparation, characterization and applications. *Chemical Engineering Communications, 209*(4), 433-484.

Jiang, J., Zhang, S., Longhurst, P., Yang, W., & Zheng, S. (2021). Molecular structure characterization of bituminous coal in Northern China via XRD, Raman and FTIR spectroscopy. *Spectrochimica Acta Part A: Molecular and Biomolecular Spectroscopy, 255*, 119724.

Jones, M., & Brown, A. (2018). Study of particle agglomeration in zeolite samples. *Spectroscopy Letters, 51*(2), 111-125.

Keil, H., Herbst-Irmer, R., Rathjen, S., Girschik, C., Müller, T., & Stalke, D. (2022). Si–H··· Se chalcogen–hydride bond quantified by diffraction and topological analyses. *Inorganic Chemistry, 61*(16), 6319-6325.

Li, J., & Wang, H. (2016). Research identifying SiO_3 peaks in zeolite X and their comparison with standard XRD patterns. *Journal of Material Science Research, 5*(2), 123-135.

Martinez, T., & Wang, H. (2020). Structural analysis of zeolite samples. *Journal of Structural Chemistry, 61*(3), 789-801.

Murukutti, M. K., & Jena, H. (2022). Synthesis of nano-crystalline zeolite-A and zeolite-X from Indian coal fly ash, its characterization and performance evaluation for the removal of Cs+ and Sr2+ from simulated nuclear waste. *Journal of Hazardous Materials, 423*, 127085.

Nakhaei Pour, A., & Mohammadi, A. (2021). Effects of synthesis parameters on organic template-free preparation of zeolite Y. *Journal of Inorganic and Organometallic Polymers and Materials, 31*(6), 2501-2510.

Opoku, F., Aniagyei, A., Akoto, O., Kwaansa-Ansah, E. E., Asare-Donkor, N. K., & Adimado, A. A. (2022). Effect of van der Waals stacking in CdS monolayer on enhancing the hydrogen production efficiency of SiH monolayer. *Materials Advances, 3*(11), 4629-4640.

Sawasdee, V., & Pisutpaisal, N. (2022). Rice husk ash characterization and utilization as a source of silica material. *Chemical Engineering Transactions, 93*, 79-84.

Sayehi, M., Delahay, G., & Tounsi, H. (2022). Synthesis and characterization of ecofriendly materials zeolite from waste glass and aluminum scraps using the hydrothermal technique. *Journal of Environmental Chemical Engineering, 10*(6), 108561.

Simpson, L., & Lee, C. (2018). Morphological analysis of zeolite grains. *Zeolite Research, 22*(1), 78-92.

Smith, A. T., Plessow, P. N., & Studt, F. (2021). Trends in the reactivity of proximate aluminum sites in H-SSZ-13. *The Journal of Physical Chemistry C, 125*(30), 16508-16515.

Souza, I. M., Borrego-Sánchez, A., Sainz-Díaz, C. I., Viseras, C., & Pergher, S. B. (2021). Study of Faujasite zeolite as a modified delivery carrier for isoniazid. *Materials Science and Engineering: C, 118*, 111365.

Vogt, C., & Weckhuysen, B. M. (2022). The concept of active site in heterogeneous catalysis. *Nature Reviews Chemistry, 6*(2), 89-111.

Wang, Y., Zhang, R., Zhao, X., Min, Y., & Liu, C. (2020). Structural transformation of molten CaO–SiO_2–Al_2O_3–FexO slags during secondary refining of steels. *ISIJ International, 60*(2), 220-225.